Quantitative Translation of Microfluidic Transporter *in Vitro* Data to *in Vivo* Reveals Impaired Albumin-Facilitated Indoxyl Sulfate Secretion in Chronic Kidney Disease

Thomas K. van der Made,[†] Michele Fedecostante,[‡] Daniel Scotcher,[†] Amin Rostami-Hodjegan,[†,⊥] Javier Sastre Toraño,[§] Igor Middel,[‡] Andries S. Koster,[‡] Karin G. Gerritsen,[¶] Vera Jankowski,[#] Joachim Jankowski,[#,∥] Joost G. J. Hoenderop,[□] Rosalinde Masereeuw,*,[‡,○] and Aleksandra Galetin*,[†,○]

[†]Centre for Applied Pharmacokinetic Research, School of Health Sciences, The University of Manchester, Manchester M13 9PL, U.K.

[‡]Division of Pharmacology, Utrecht Institute for Pharmaceutical Sciences and [§]Department of Chemical Biology and Drug Discovery, Utrecht Institute for Pharmaceutical Sciences, Utrecht University, Utrecht 3584 CG, The Netherlands

[⊥]Simcyp Division, Certara UK Limited, Sheffield S1 2BJ, U.K.

[¶]Department of Nephrology and Hypertension, University Medical Center Utrecht, Utrecht 3508 GA, The Netherlands

[#]Institute for Molecular Cardiovascular Research, RWTH Aachen University Hospital, Aachen 52074, Germany

[∥]School for Cardiovascular Diseases, Maastricht University, Universiteitssingel 50, Maastricht 6229 ER, The Netherlands

[□]Department of Physiology, Radboud Institute for Molecular Life Sciences, Radboud University Medical Center, Nijmegen 6500 HB, The Netherlands

S *Supporting Information*

ABSTRACT: Indoxyl sulfate (IxS), a highly albumin-bound uremic solute, accumulates in chronic kidney disease (CKD) due to reduced renal clearance. This study was designed to specifically investigate the role of human serum albumin (HSA) in IxS renal secretion via organic anion transporter 1 (OAT1) in a microfluidic system and subsequently apply quantitative translation of *in vitro* data to predict extent of change in IxS renal clearance in CKD stage IV relative to healthy. Conditionally immortalized human proximal tubule epithelial cells overexpressing OAT1 were incubated with IxS (5−200 μM) in the HSA-free medium or in the presence of either HSA or CKD-modified HSA. IxS uptake in the presence

of HSA resulted in more than 20-fold decrease in OAT1 affinity ($K_{m,u}$) and 37-fold greater *in vitro* unbound intrinsic clearance ($CL_{int,u}$) versus albumin-free condition. In the presence of CKD-modified albumin, $K_{m,u}$ increased four-fold and IxS $CL_{int,u}$ decreased almost seven-fold relative to HSA. Fold-change in parameters exceeded differences in IxS binding between albumin conditions, indicating additional mechanism and facilitating role of albumin in IxS OAT1-mediated uptake. Quantitative translation of IxS *in vitro* OAT1-mediated $CL_{int,u}$ predicted a 60% decrease in IxS renal elimination as a result of CKD, in agreement with the observed data (80%). The findings of the current study emphasize the role of albumin in IxS transport via OAT1 and explored the impact of modifications in albumin on renal excretion via active secretion in CKD. For the first time, this study performed quantitative translation of transporter kinetic data generated in a novel microfluidic *in vitro* system to a clinically relevant setting. Knowledge gaps and future directions in quantitative translation of renal drug disposition from microphysiological systems are discussed.

KEYWORDS: *indoxyl sulfate, OAT1, proximal tubule, in vitro−in vivo extrapolation, CKD*
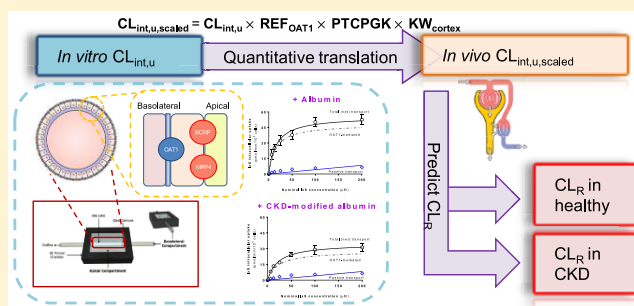
INTRODUCTION

Chronic kidney disease (CKD) is a global health care problem, affecting approximately 12% of the population worldwide, with a prevalence of around 6.5% in advanced CKD stages III−V.[1,2] CKD results in the accumulation of uremic solutes in plasma, especially protein-bound toxins secreted by renal drug

transporters.[3] One of the most prevalent accumulated solutes is indoxyl sulfate (IxS), implicated as a contributor to cardiovascular disease[4] and renal disease progression.[5] The underlying mechanisms causing reduced renal plasma excretion clearance (CL_R) and accumulation of IxS (also of drugs given to CKD patients) are still not fully elucidated. Intact nephron hypothesis proposes that the number of functional nephrons is decreased in CKD and that glomerular filtration rate (GFR) and residual tubular function decrease in parallel.[6] When tubular secretion is the dominant route of uremic toxin/drug elimination, impaired active secretion via renal drug transporters associated with CKD is expected to contribute significantly to reduced CL_R.[3,7]

IxS is actively secreted via basolaterally expressed organic anion transporters (OAT) 1 and, to a lesser extent, OAT3,[8−11] paired with efflux via MRP4, BCRP, and OAT4 transporters at the apical proximal tubule membrane.[12,13] In plasma of healthy subjects, this uremic solute is >90% bound to human serum albumin (HSA), with minimal binding to other plasma proteins.[14] In CKD, the extent of IxS binding to albumin is reduced, and this is attributed not only to changes in albumin concentrations but also competition for albumin binding site and potentially post-translational modifications of the protein.[15−17] In healthy subjects, mean total and free IxS concentrations range from 0.4−0.9 mg/L (1.9−4.2 μM) and 0.02−0.03 mg/L (0.09−0.13 μM), respectively (Table S1). In advanced CKD (stage IV+), both total (average 24 mg/L; 113 μM) and free (average 2.4 mg/L; 11.3 μM) IxS concentrations increase (Table S1).

Considering all these changes in CKD, it is important to delineate the role of albumin in tubular secretion of IxS, in particular considering proposed albumin-facilitated active transport via OATs.[11,18] Jansen et al. recently developed a microfluidic system wherein human conditionally immortalized proximal tubule epithelial cells (ciPTEC) were seeded on a hollow fiber membrane.[11,19] Use of microfluidic system and ability to investigate transepithelial transport were envisaged to improve mechanistic *in vitro* characterization of the complex interplay between multiple processes affecting renal drug disposition, namely basolateral and apical uptake and efflux transporters, passive diffusion, and tubular reabsorption. Other advantages of this microfluidic system include recapitulation of the extracellular environment, cell-to-medium ratio, tubule formation, and removal of waste metabolites.

Quantitative translation of transporter data generated *in vitro* to *in vivo* is often done using physiologically based pharmacokinetic modeling (PBPK).[20−23] *In vitro−in vivo* extrapolation (IVIVE) of transporter kinetic data accounts for differences in expression of drug transporters or activity between the cellular system and *in vivo*.[22,24] Although well-established approach for a number of cellular systems,[25] the translational ability of data from novel microphysiological systems[26,27] is yet to be ascertained.

There is an increasing interest to use IVIVE-based PBPK models to support dosage adjustments recommendations in product labeling for specific populations.[22,28−30] However, examples where PBPK modeling was used to explore implications of different underlying disease mechanisms on predicted drug pharmacokinetics are still sparse. In the case of renal impairment, physiological kidney models have investigated the impact of reduced proximal tubule cellularity and reduced transporter expression, in conjunction with well-

defined changes in GFR and plasma protein binding, on the predicted CL_R of selected drugs.[31−33]

This study aimed to understand the role of albumin in IxS renal secretion via OAT1 in both healthy population and in advanced stage of CKD. To that end, IxS tubular secretion in the microfluidic system was investigated under different albumin conditions *in vitro* and quantitatively translated to *in vivo*; the predicted extent of change in IxS CL_R in CKD relative to healthy was compared with reported clinical data.

■ EXPERIMENTAL SECTION

Chemicals and Materials. All chemicals and HSA were purchased from Sigma-Aldrich (Zwijndrecht, The Netherlands). MicroPES TF10 hollow fiber capillary membrane (wall thickness 100 ± 25 μm, inner diameter 300 ± 40 μm, max pore size 0.5 ± 0.1 μm) was purchased from 3 M − Membrana GmbH (Wuppertal, Germany). CKD-modified HSA has undergone post-translational modifications by guanidinylation reflecting changes occurring in CKD patients, as described previously.[15]

Uptake of Indoxyl Sulfate by ciPTEC-OAT1 in Microfluidic System. ciPTEC with stable overexpression of OAT1 (ciPTEC-OAT1)[34] was cultured in supplemented PTEC media under static conditions before seeding (between passage number 29−43).[35] Hollow fiber capillary membrane was coated with L-DOPA and collagen type IV and seeded (1.5 × 10^6 cells), analogous to previous protocol.[19]

ciPTEC-OAT1 cells were exposed to a range of IxS concentrations (5−200 μM) in the microfluidic system (detailed information on system has been reported previously)[19] for 5 min at a flow rate of 6 mL h^{-1}. IxS was dissolved in Kreb-Henseleit buffer (supplemented with 10 mM Hepes, pH = 7.4), and uptake was performed in the presence and absence of potent OAT inhibitor probenecid (500 μM). Efflux transporter activity (e.g., BCRP and MRP4) was inhibited by addition of inhibitors (KO143 and MK571, 5 μM) in the apical compartment. Active uptake of IxS was investigated under three conditions, namely in albumin-free medium, with HSA at 1 mM (corresponding to a physiological plasma albumin concentration in humans, 35−50 g/L),[11] and in the presence of CKD-modified HSA at 1 mM. Uptake was terminated by addition of ice-cold Kreb-Henseleit buffer. The buffer was removed, and cells were lysed with 250 μL of 0.1 M NaOH for 15 min. Subsequently, intracellular concentrations of IxS were quantified by liquid chromatography−tandem mass spectrometry (LC−MS/MS; Supporting Information). The IxS fraction unbound in incubation media (fu_{med}) was determined by measuring IxS free and bound fractions using ultrafiltration over the concentration range tested, as described previously.[11,15]

Transepithelial Transport Studies. ciPTEC-OAT1 cells in the microfluidic system were perfused with uremic plasma (measured IxS concentration of 282 ± 4 μM) or healthy plasma (spiked with 282 μM IxS) for 10 min in the presence or absence of probenecid (500 μM). After perfusion, fluid in the apical compartment was collected and IxS was quantified by LC−MS/MS (Supporting Information). Cell viability (Prestoblue cell viability assay) and barrier integrity (inulin-FITC leakage) assays were performed using cisplatin (200 μM) as a positive control. Cisplatin was used as positive control as it is known to be toxic to kidney cells and disrupts integrity of membrane barrier. Pooled uremic and healthy plasma samples from subjects were obtained from the Department of
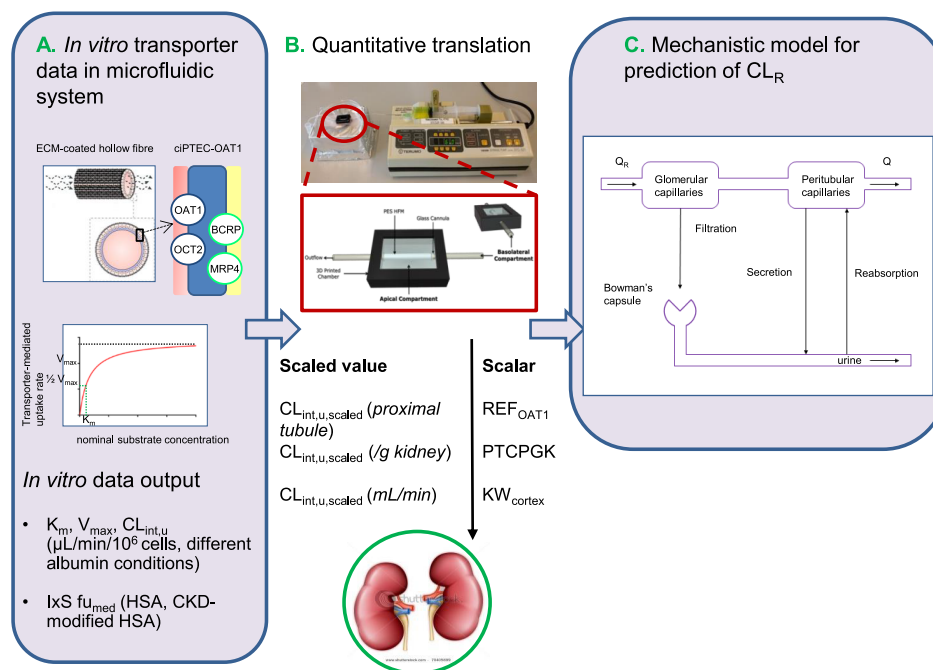
Figure 1. Quantitative translation of *in vitro* transporter kinetic data obtained in microfluidic system to predict renal plasma excretion clearance (CL_R). (A) Indoxyl sulfate (IxS) uptake was investigated in a microfluidic device with ciPTEC-OAT1 and *in vitro* unbound intrinsic clearance ($CL_{int,u}$) was determined. (B) $CL_{int,u}$ was scaled with relative OAT1 expression factor (REF_{OAT1}), the number of proximal tubule cells per gram of kidney (PTCPGK) and cortex kidney weight (KW_{cortex}) to predict *in vivo* unbound intrinsic clearance ($CL_{int,u,scaled}$). (C) To predict renal plasma clearance (CL_R) of IxS, other renal processes (glomerular filtration and tubular reabsorption) were also accounted for (eq 5). The filtration component is determined by the glomerular filtration rate (GFR) and the fraction unbound of IxS (fu_p) in plasma. Q_R represents the renal cortex blood flow.

Nephrology and Hypertension, University Medical Center Utrecht, Utrecht, The Netherlands.

Data Analysis. IxS uptake rates (pmol/min/10^6 cells) in the presence and absence of probenecid were calculated by normalizing measured uptake amounts for incubation time, assuming linearity with respect to time and fiber cellularity (details on determination of the cell number in Table S2). Passive transport was determined assuming that probenecid (500 μM) completely inhibited uptake via OAT1. OAT1-mediated uptake rate (pmol/min/10^6 cells) at specific IxS concentration was calculated as a difference between total and passive transport rates.

The Michaelis constant defining OAT1 binding affinity (K_m; μM) and maximum uptake rate (V_{max}; pmol/min/10^6 cells) were estimated by fitting the Michaelis–Menten eq (eq 1) to OAT1-mediated uptake rates and nominal IxS concentrations using Graphpad Prism 7.04 (La Jolla California USA). IxS fu_{med} was calculated as the slope of the linear regression of the nominal versus free IxS concentration (Figure S1). Subsequently, the K_m corrected for binding ($K_{m,u}$) and *in vitro* unbound intrinsic clearance ($CL_{int,u}$) expressed in μL/min/10^6 cells were calculated (eqs 2 and 3):

$$v = \frac{V_{max} \times [S]}{K_m + [S]} \quad (1)$$

$$K_{m,u} = K_m \times fu_{med} \quad (2)$$

$$CL_{int,u} = \frac{V_{max}}{K_{m,u}} \quad (3)$$

Quantitative Translation of *in Vitro* Unbound Intrinsic Clearance to *in Vivo*. IVIVE was performed by applying physiological scaling factors[36] to translate *in vitro* IxS kinetic data obtained in a microfluidic system to an organ level (eq 4, Figure 1):

$$CL_{int,u,scaled} = CL_{int,u}[\mu L/min/10^6 \text{ cells}]$$

$$\times REF_{OAT1}\left[\frac{\frac{\text{pmolTransporter PTC}}{10^6 \text{PTC}}}{\frac{\text{pmolTransporter system}}{10^6 \text{cells of system}}}\right]$$

$$\times PTCPGK\left[\frac{10^6 \text{PTC}}{\text{g Kidney}}\right] \times KW_{cortex}[\text{g kidney}] \quad (4)$$

$CL_{int,u}$ is derived from *in vitro* IxS uptake studies and reflects OAT1-mediated IxS uptake, whereas $CL_{int,u,scaled}$ represents the scaled *in vivo* unbound OAT1-mediated intrinsic clearance, assuming that uptake via OAT1 is the rate-determining step in IxS renal disposition. REF_{OAT1} is relative expression factor for OAT1 (dimensionless) and accounts for differences in transporter expression between different systems. Because of the lack of data on OAT1 expression in ciPTEC in the microfluidic system, REF_{OAT1} value of 1 was applied assuming no difference in OAT1 expression between *in vitro* and *in vivo*, as done previously.[31] PTCPGK (number of proximal tubule cells/g kidney) allows the extrapolation of *in vitro* data to per g of kidney.[25,36] A mean value of 60 million of proximal tubule cells/g kidney was based on previous studies.[32,36] The ratio between ciPTEC cellularity and primary proximal tubule cells was assumed to be 1, as used before for HEK293 cells.[36] Final scaling factor (cortex kidney weight, KW_{cortex}) extrapolates active clearance value to both kidneys; focus was on cortex as proximal tubule cells exclusively reside in this region.

Table 1. Information on Scaling Factors Used To Predict *in Vivo* Unbound OAT1-Mediated Intrinsic Clearance ($CL_{int,u,scaled}$) and Indoxyl Sulfate Renal Plasma Excretion Clearance (IxS CL_R)[a]

	healthy subjects	CKD stage IV	ref
IVIVE scaling factors			
REF_{OAT1}	1 (assumed)	1 (assumed)[b]	
PTCPGK (proximal tubule cells/g kidney)	60×10^6 (range $50-70 \times 10^6$)	60×10^{6b}	Neuhoff et al.[36]
kidney weight (g) (average left + right kidney)	249	249[b]	Molina et al.[45,46] and taking into account male/female ratio in study by Poesen et al.[47]
KW_{cortex} (g)	169 (68% of kidney weight)	169 (68% of kidney weight)[b]	Scotcher et al.[48]
Input in Static Model To Predict IxS CL_R			
Q_R (mL/min)	1008	585	Scotcher et al.[48] and 42% reduction in advanced CKD patients (Table S3)
GFR (mL/min) (defined GFR category)	105 (90−120)	22.5 (15−30)	CKD work group[49]
fu_p	0.025	0.06	Rossi et al.[44]
$R_{B:P}$	0.55 (1-hematocrit, assumed)	0.66 (1-hematocrit, assumed)	Rowland Yeo et al.[42] and taking into account male/female proportionality in study Poesen et al.[47]
F_{reab}	0 (assumed)	0 (assumed)	
$CL_{int,u,scaled}$ (mL/min)	342.5	52.0	

[a]Reported numbers are based on physiological values (e.g. PTCPGK, KW_{cortex}, Q_R, and fu_p), experimental values (ciPTEC number and $CL_{int,u}$), or were assumed due to lack of clinical or experimental evidence (REF_{OAT1}, $R_{B:P}$, and F_{reab}). Differences in individual parameters in healthy subjects and CKD patients were taken into account if clinical evidence was available. [b]No quantitative information available on differences between healthy subjects and CKD patients for these parameters.

Considering uncertainty in some of the scaling factors, sensitivity analysis was performed by varying REF_{OAT1} and PTCPGK in the model for healthy subjects to assess the impact on predicted IxS CL_R.

In the case of advanced CKD (stage IV), quantitative translational approach followed the same principles as above for healthy; known changes in physiological parameters (e.g., GFR, fu_p) associated with the disease were considered (Table 1). Scaling factors (PTCPGK, REF_{OAT1}) were the same as in healthy population due to lack of quantitative data on cell number or transporter expression in CKD patients. Subsequently, impact of disease-related reduction in either transporter expression or PTCPGK on the predicted CL_R ratio was investigated. The implemented decrease in these physiological scaling factors was proportional to changes in GFR in CKD stage IV based on intact nephron hypothesis and animal studies reporting proximal tubule cell damage, reduced kidney size, and reduced OAT expression in this disease.[7,37−39] Model input values for the individual parameters are summarized in Table 1.

Prediction of Indoxyl Sulfate Renal Plasma Excretion Clearance. To predict total IxS CL_R, three renal elimination mechanisms were considered, namely glomerular filtration, active secretion, and tubular reabsorption, derived from Zamek-Gliszczynski et al.[40] and adapted to estimate renal plasma clearance (eq 5):[41]

$$CL_R = \left[fu_p \times GFR + \left(1 - \frac{fu_p \times GFR}{Q_R} \right) \times \left(\frac{Q_R \times fu_p \times CL_{int,u,scaled}}{Q_R + \frac{fu_p}{R_{B:P}} \times CL_{int,u,scaled}} \right) \right] \times (1 - F_{reab}) \quad (5)$$

where Q_R is the renal cortex blood flow (mL/min), $CL_{int,u,scaled}$ (mL/min) is the *in vivo* unbound intrinsic clearance (defined

in eq 4), fu_p is fraction unbound in plasma, and F_{reab} is the fractional tubular reabsorption. $R_{B:P}$ is the IxS blood-to-plasma ratio, and a value of 0.55 (1-hematocrit) was applied due to lack of reported data. Eq 5 can be expressed in terms of blood clearance, assuming equilibrium of unbound concentrations in plasma and blood.[40]

Relative contribution of active secretion to IxS CL_R was calculated (eq 6):

$$\text{Relative contribution (\%)} = \left(1 - \frac{GFR \times fu_p}{CL_R} \right) \times 100 \quad (6)$$

Contribution of tubular reabsorption was assumed to be negligible ($F_{reab} = 0$). Potential involvement of OAT4 as apical uptake transporter was not considered in this study. Eq 5 was used to calculate CL_R for healthy and in the case of CKD changes in physiological parameters associated with CKD were considered (Table 1). Although reported differences in hematocrit levels between healthy and CKD[42] were accounted for, these had no impact on the predicted CL_R value.

Collation of Indoxyl Sulfate Clinical Data in Healthy and CKD Population. Predicted IxS CL_R was compared to reported clinical data to validate the predictive performance and translational ability of the *in vitro* data generated in the current study. Pubmed was searched for clinical studies reporting (unbound) CL_R of IxS in healthy subjects and in patients with varying stages of CKD (Table 4). Clinical studies with end stage renal disease, hemodialysis, or peritoneal dialysis patients were excluded from the analysis unless IxS free and total levels were determined before dialysis. Tables 3 and S1 give an overview of clinical studies (after 2012) reporting total or free IxS concentrations in healthy subjects and CKD patients.[43] The fu_p value from Rossi et al.[44] for CKD stage IV was used as input in the CL_R prediction model since the study reported values per specific CKD stage.
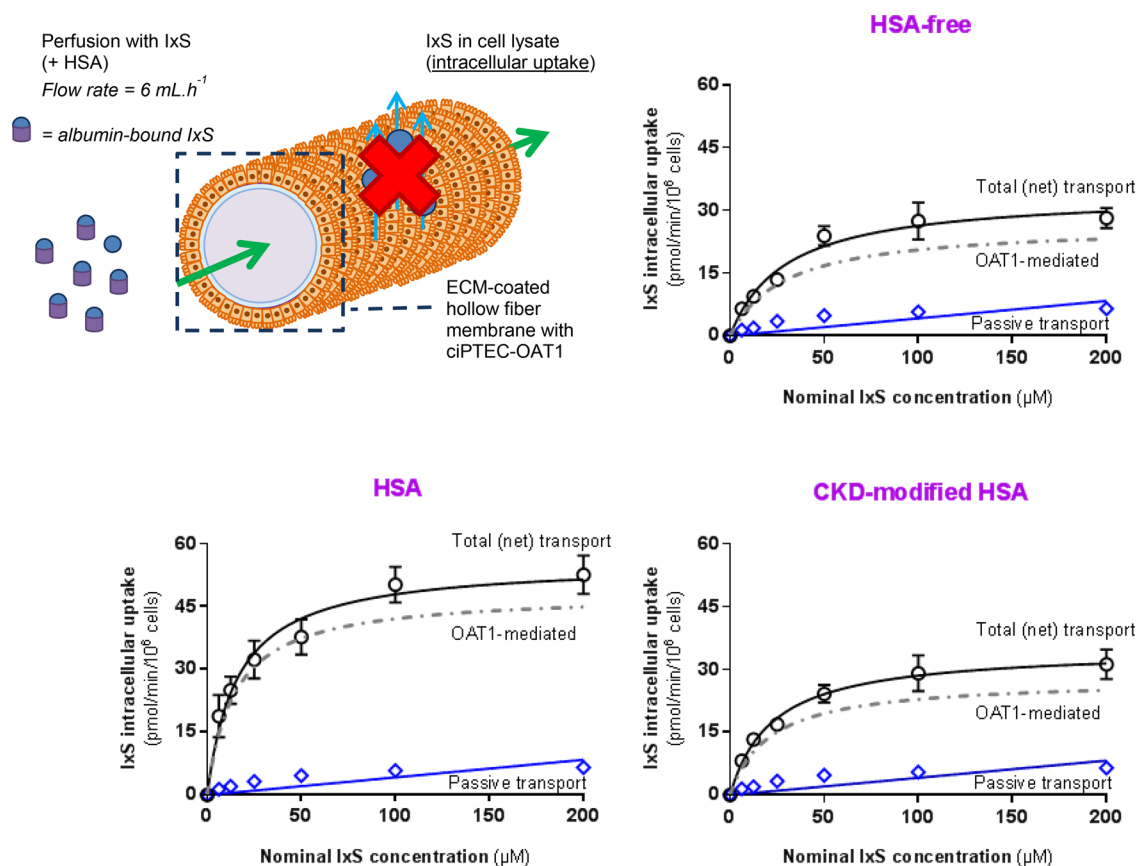
Figure 2. Indoxyl sulfate (IxS) uptake kinetics in ciPTEC-OAT1 seeded in microfluidic system in the absence or presence of human serum albumin (HSA) or CKD-modified albumin. ciPTEC-OAT1 cells were exposed to a range of IxS concentrations (5−200 μM) in HSA-free incubation media (HSA-free), in the presence of 1 mM HSA (corresponding to healthy plasma) and in the presence of 1 mM CKD-modified HSA. Top left panel illustrates the experimental design to determine intracellular IxS uptake; efflux transporter activity was inhibited by addition of inhibitor cocktail in the apical compartment (ECM = extracellular matrix). Observed total transport (open black circle) and passive transport (open blue diamonds) are depicted. Fitted Michaelis−Menten equation to OAT1-mediated transport data (dashed gray line) is shown. Linear regression of passive transport is represented by the blue solid line. Data are shown as mean $\pm$ SD of three independent experiments.

Table 2. *In Vitro* Organic Anion Transporter 1 (OAT1) Kinetic Parameters for Indoxyl Sulfate (IxS) and Corresponding Fraction Unbound in Incubation Medium (fu$_{med}$) in Different Human Serum Albumin (HSA) Conditions Investigated[a]

albumin condition used	V$_{max}$ (pmol/min/10^{6}cells)	K$_m$(μM)	K$_{m,u}$ (μM)[b,c]	IxS fu$_{med}$	IxS CL$_{int,u}$[d](μL/min/10^6 cells)	CL$_{int,u,scaled}$[e,f,g](mL/min)
HSA-free	26.5 ± 2.2	29.3 ± 7.5	29.3	1	0.90	9.2
+HSA	48.1 ± 2.5	14.4 ± 2.9	1.4	0.1	33.7	342.5
+CKD-modified HSA	27.7 ± 1.0	21.0 ± 2.5	5.4	0.26	5.1	52.0

[a]IxS uptake was investigated in the absence of HSA (HSA-free), in the presence of HSA, and in the presence of CKD-modified HSA. Values are presented as mean $\pm$ SD of three independent experiments. [b]K$_m$ corrected by measured fu$_{med}$ (K$_m$ × fu$_{med}$ = K$_{m,u}$). IxS fu$_{med}$ was 0.1 (albumin) and 0.26 in CKD-modified albumin condition. [c]K$_{m,u}$ (μM) equivalent to 6.2 (HSA-free), 0.3 (HSA), and 1.2 mg/L (CKD-modified HSA). [d]CL$_{int,u}$ obtained as V$_{max}$/K$_{m,u}$. [e]Scaling factors used: REF$_{OAT1}$ = 1; PTCPGK = 60 × 10^6 cells/g kidney; and KW$_{cortex}$ = 169 g. [f]Used as input in CL$_R$ prediction model (eq 5) in healthy subject population (HSA-free and HSA *in vitro* conditions) and in CKD stage IV population (CKD-modified HSA *in vitro* condition). Predicted CL$_R$ was 2.9, 11.0, and 4.4 mL/min for HSA-free, HSA, and CKD-modified HSA, respectively. [g]Relative contribution of OAT1-mediated active secretion clearance to CL$_R$ was 8.0, 76, and 70% for HSA-free, HSA, and CKD-modified HSA, respectively.

■ RESULTS

OAT1-Mediated Uptake of Indoxyl Sulfate in Microfluidic System $\pm$ Albumin. Concentration-dependent uptake of IxS by ciPTEC-OAT1 monolayers was observed in HSA-free medium; this trend was also evident in the presence of albumin (Figure 2, Table 2). Saturable uptake of IxS in HSA-free medium resulted in K$_m$ and V$_{max}$ of 29.3 μM and 26.5 pmol/min/10^6 cells, respectively (Table 2). The IxS fu$_{med}$ in the presence of HSA was 0.1 (Figure S1). The presence of HSA resulted in increased transporter affinity and 20-fold lower K$_{m,u}$ compared to albumin-free incubation media. In

addition, the presence of albumin increased the transporter V$_{max}$, and as a result, the IxS OAT1-mediated CL$_{int,u}$ increased by 37-fold (Table 2). The inclusion of albumin did not have an impact on IxS passive diffusion (Figure 2).

OAT1-Mediated Uptake of Indoxyl Sulfate in Presence CKD-Modified Albumin. Concentration-dependent uptake of IxS in ciPTEC-OAT1 was observed in the presence of CKD-modified HSA (Figure 2, Table 2). A lower extent of IxS binding was apparent in the presence of CKD-modified HSA, with a fu$_{med}$ of 0.26 relative to 0.1 in the HSA condition (Figure S1). Nearly four-fold lower affinity for OAT1 and

Table 3. Studies Reporting Indoxyl Sulfate Fraction Unbound in Plasma (IxS fu$_p$) in CKD Patients and Healthy Subjects[a]

population	n	mean GFR (mL/min)	serum IxS total (mg/L)[b]	serum IxS free (mg/L)[b]	IxS fu$_p$	ref
CKD Patients						
prevalent hemodialysis patients	1273	NR	25 ± 12	2.7 ± 1.9	0.11	Shafi et al.[50]
hemodialysis patients	14	NR	19 (10, 23)	1.3 (0.6, 1.7)	0.07	Camacho et al.[51]
patients with CKD stage IV or V (nondialyzed)	37	24 ± 8	3.8 (2.6−5.8)	0.15 (0.09−0.2)	0.04	Rossi et al.[52]
stable CKD patients on peritoneal dialysis	15	NR	7.6 ± 5.3	0.7 ± 0.4	0.09	Eloot et al.[53]
patients on initiation of maintenance dialysis therapy in the preceding 3 months	394	NR	17.1 ± 10.2	1.3 ± 1.0	0.07	Shafi et al.[54]
patients with varying stages of CKD	327	46 ± 25	2.8 (1.5−12.1)	0.11 (0.04−2.1)	0.04	Rossi et al.[44]
patients on hemodialysis	20	NR	35 ± 9	3.6 ± 2.3	0.10	Sirich et al.[55]
	20	NR	32 ± 12	2.8 ± 1.6	0.09	
CKD stage V not undergoing hemodialysis	40	13 ± 6	11.6 (10.9)	1 (1.23)	0.09	Wu et al.[56]
patients on peritoneal dialysis	46	NR	41 ± 16	4.3 ± 2.6	0.11	Lin et al.[57]
uremic toxin workgroup			37 ± 27	3.8 ± 2.5	0.10	Eutox database[58]
weighted mean advanced CKD			24 ± 13[c]	2.4 ± 2.0[c]	0.10	
Healthy Subjects						
healthy subjects	5	142 ± 22	NR	0.03 ± 0.01	0.03	Sirich et al.[59]
healthy subjects	42	93 ± 12	0.9 (0.4−1.5)	0.02 (0.02−0.02)	0.03	Rossi et al.[44]
healthy subjects			0.54 ± 4.0			Eutox database[58]

[a]Values in the studies were reported as median (interquartile range) or mean ± SD. More detailed information on study characteristics (e.g. albumin levels, IxS detection method, and time of sampling) can be found in Table S1 as well as additional studies only reporting IxS total concentrations. NR = not reported. [b]To convert value in mg/L to μM for IxS: value × 1000/213 (molecular weight of IxS). [c]Studies included in the weighted mean if subjects in the study had advanced stage of CKD (e.g., stage IV/V). In addition, if mean value ± standard deviation was reported.

Table 4. Studies Reporting Indoxyl Sulfate Renal Plasma Excretion Clearance (IxS CL$_R$) in CKD Patients and Healthy Subjects[a]

population	n	mean GFR (mL/min)	IxS CL$_R$ (mL/min)	% active renal secretion[b]	total serum concentrations of IxS (mg/mL)	IxS fu$_p$	ref
CKD Patients							
CKD patients (across all stages)	291	41.1 (28.1−63.1)	20.2 (12.3−34.8)	88	3.2 (1.9−4.9)		Suchy-Dicey et al.[60]
CKD patients (across all stages)	203	34.3 (23.1−55.9)	17.7 (9.4−33.2)	88	2.04 (1.09−4.0)		Poesen et al.[47]
GFR and CL$_R$ values used in this study		22.5	12.5[c]				
Healthy Subjects							
overweight, but otherwise healthy	25	117 ± 14	67 ± 28	96	0.90 ± 0.42		Rivara et al.[61]
subjects with normal renal function	5	142 ± 22	53 ± 7	93	NR	0.03	Sirich et al.[59]
GFR and CL$_R$ values used in this study		105	67.8[c]				

[a]Values in the studies were reported as median (interquartile range) or mean ± SD. NR = not reported. [b]Active renal secretion clearance calculated as CL$_R$ − fu$_p$ × GFR. fu$_p$ value of 0.025 was used for healthy subjects and 0.06 for CKD stage IV patients. [c]IxS CL$_R$ calculated using correlation between GFR and IxS CL$_R$ reported by Poesen et al.[47]

reduced V$_{max}$ in the presence of CKD-modified HSA (Table 2) resulted in 6.6-fold decrease in CL$_{int,u}$ relative to HSA (Table 2). Passive diffusion between different albumin conditions was comparable (Figure 2).

Clinical Studies Reporting Indoxyl Sulfate Fraction Unbound in Plasma in Healthy Subjects and CKD Patients. Table 3 provides an overview of collated studies reporting IxS fu$_p$, whereas all collated literature studies reporting total IxS concentrations in plasma are summarized in Table S1. High intra- and inter-study variability in total and free IxS concentrations were apparent, in line with pre-2012 data reported by the uremic toxin workgroup (Table 3).[43] One study reported fu$_p$ values in various CKD stages and found a substantial increase in fu$_p$ with increasing severity of the

disease (from 0.03 to 0.16 in control to- stage V, respectively).[44]

Studies Reporting Indoxyl Sulfate CL$_R$ in CKD Patients and Healthy Subjects. A limited number of studies reporting actual IxS CL$_R$ were available (Table 4). Weighted mean of IxS CL$_R$ values reported in healthy subjects was 65 ± 26 mL/min. Across a CKD population, study average CL$_R$ values ranged from 17.7 to 20.2 mL/min (Table 4). Average GFR values in these cohorts were 34.3 and 41.1 mL/min, respectively. Clinical IxS CL$_R$ values for both healthy and advanced CKD (stage IV) for further analysis were taken from Poesen et al.[47] since a correlation between a GFR range and IxS CL$_R$ was reported (e.g., CL$_R$ = 0.67 × GFR − 2.57, R^2 = 0.55). This allowed calculation of IxS CL$_R$ for specific stages of CKD. Considering that CKD stage IV is defined by a GFR

Table 5. Sensitivity Analysis Performed in Healthy Subjects To Assess Impact of Uncertainty in Model Input Parameters (e.g., Relative OAT1 Expression Factor (REF_{OAT1}) and Proximal Tubule Cells Per g of Kidney (PTCPGK))[a]

GFR (mL/min)	REF_{OAT1} (dimensionless)	PTCPGK (10^6 cells/g kidney)	IxS $CL_{int,u,scaled}$ (mL/min)	IxS CL_R (mL/min)
Sensitivity Analysis in PTCPGK				
105	1	30	171	6.9
105	1	40	228	8.3
105	1	50	285	9.7
105	1	60	343	11.0
105	1	70	400	12.4
105	1	80	457	13.8
105	1	120	685	19.2
Sensitivity Analysis in REF_{OAT1}				
105	0.25	60	86	4.8
105	0.33	60	114	5.5
105	0.5	60	171	6.9
105	1	60	343	11.0
105	2	60	685	19.2
105	3	60	1027	27.1
105	4	60	1370	34.8

[a]Predictions were performed in healthy subjects by varying systems parameters from values of 1.00 (REF_{OAT1}) and 60 (PTCPGK) used as a starting point. 0.25−4 (REF_{OAT1}) and 30−120 × 10^6 cells/g kidney (PTCPGK) were explored. Remaining physiological system parameters are as defined in Table 1 for healthy population.

Table 6. Impact of Changes in Physiologically-Based Scaling Factors (REF_{OAT1} or PTCPGK) in CKD Population on Predicted Indoxyl Sulfate Renal Plasma Excretion Clearance Relative to Healthy

GFR (mL/min)	REF_{OAT1}[a]	PTCPGK[a] (10^6 cells/g kidney)	IxS $CL_{int,u,scaled}$ (mL/min)	IxS CL_R (mL/min)	predicted decrease in CL_R in CKD relative to healthy (%)
22.5	1.00	60.0	52.0	4.4	60
22.5	0.25 (75%)	60.0	13.0	2.1	81
22.5	1.00	15.0 (75%)	13.0	2.1	81

[a]If shown, number in brackets represents decrease in the scaling factor in CKD population relative to healthy. Remaining physiological system parameters used for prediction in CKD are as defined in Table 1.
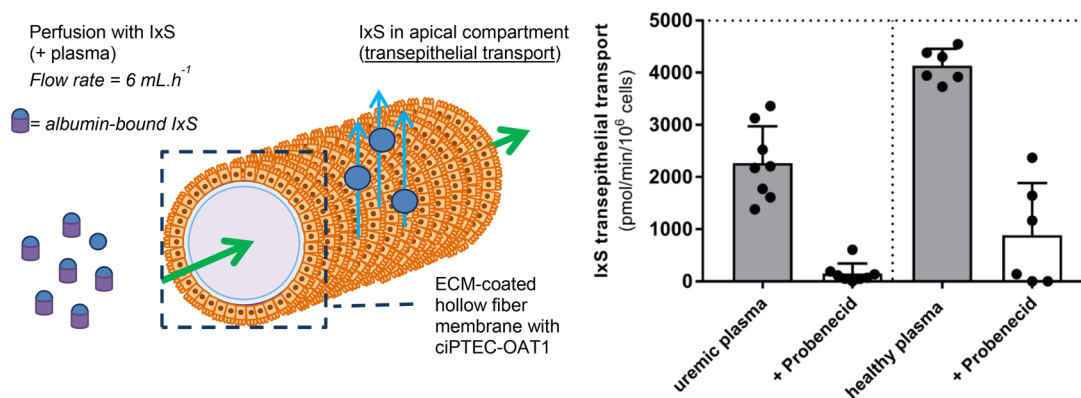
Figure 3. Active secretion of indoxyl sulfate (IxS) in ciPTEC-OAT1 cells in the microfluidic system exposed to either healthy plasma or uremic plasma. Panel on the left illustrates the experimental design to determine IxS transepithelial transport in the microfluidic system (ECM = extracellular matrix). ciPTEC-OAT1 cells were perfused with human plasma samples for 10 min at flow rate of 6 mL h^{-1}. The panel on the right depicts transepithelial transport of IxS when incubated in the presence of uremic plasma (282 ± 4 μM) or healthy plasma spiked with IxS (282 μM) in the absence or presence of probenecid (500 μM). Data are shown as mean ± SD of at least three independent experiments (performed in duplicate). High variability between individual experiments was evident and may be related to inconsistency in barrier integrity in different experiments. In addition, the efficacy of probenecid in the basolateral compartment may have been affected in the presence of certain plasma samples, for unknown reasons.

range of 15−30 mL/min, the midpoint of 22.5 mL/min was used to calculate the corresponding IxS CL_R value (12.5 mL/min) from linear regression. The average GFR taken for healthy subjects was 105 mL/min (range 90−120), resulting in a calculated IxS CL_R of 67.8 mL/min for this population.

Quantitative Translation of Transporter *in Vitro* Data Obtained in Presence and Absence of Albumin.

In vitro OAT1-mediated uptake clearance of IxS obtained in absence or presence of HSA or CKD-modified HSA in the incubation medium was extrapolated to *in vivo* using the physiologically based approach (eq 4 and 5) (Table 2). Predicted IxS CL_R

values in healthy subjects were 11.0 mL/min and 2.9 mL/min following translation of *in vitro* transporter data in presence of HSA versus absence of HSA, respectively.

Translation of *in vitro* OAT1-mediated $CL_{int,u}$ obtained in CKD-modified albumin condition predicted a 60% decrease in IxS CL_R in CKD stage IV relative to healthy subjects. The predicted relative contribution of active secretion to IxS CL_R was 76% in healthy subjects and 70% in CKD stage IV (Table 2). Although translational method captured disease-related decrease in IxS CL_R reasonably well (80% decrease reported clinically[47]), it was apparent that absolute IxS CL_R values in both CKD patients and healthy subjects were significantly under-predicted (observed CL_R is 12.5 and 67.8 mL/min, respectively, Table 4). To rationalize these trends and investigate the impact of uncertainty in some of the model input parameters on the predicted IxS CL_R, sensitivity analysis was performed (Table 5, range of scaling factors explored is based on reported literature[62−65]). The analysis demonstrated sensitivity of the model to PTCPGK (range tested: 30−120 × 10^6, resulting in predicted CL_R of 6.9- 19.2 mL/min) and REF_{OAT1} (range tested: 0.25−4, resulting in predicted CL_R of 4.8−34.8 mL/min). Because of lack of data in CKD, initial quantitative prediction of CL_R in CKD assumed that these physiological scaling factors do not change with disease progression, which is unlikely. Subsequent analysis where either number of proximal tubule cells or OAT1 expression (captured by REF_{OAT1}) were decreased proportionally to GFR (approximately 75% in CKD stage IV) recovered clinically observed decrease in CL_R in advanced CKD patients relative to healthy (Table 6).

Transepithelial Transport of Indoxyl Sulfate in ciPTEC-OAT1. To assess the ability of microfluidic system to capture physiological complexities of CKD, IxS transepithelial transport was investigated upon perfusion with plasma from renal healthy controls spiked with IxS (282 μM) or plasma from CKD patients with the same IxS concentration (as measured). Transepithelial transport of IxS across ciPTEC-OAT1 monolayers was evident in all conditions (Figure 3), with unaltered cell viability and barrier function (Figure S2). A 55% reduction in transepithelial transport rate was observed in the presence of uremic plasma compared to plasma from renal healthy controls spiked with IxS (2270 ± 700 vs 4140 ± 320 pmol/min/10^6 cells, Figure 3). Transepithelial transport decreased (>85%) by coperfusion with probenecid.

■ DISCUSSION

The concept of albumin-facilitated drug transport has been postulated and rationalized by the presence of membrane "albumin receptors" that facilitate uptake of highly albumin-bound drugs in hepatocytes.[66−68] Recently, a similar mechanism has been proposed for uptake via renal OAT transporters.[11,18] Clinical data in CKD patients report increased IxS accumulation and reduced extent of IxS binding to albumin in this population.[15] However, the potential role of albumin-facilitated OAT1 transport in either healthy or CKD subjects and its effect on IxS CL_R are not understood. To this end, the impact of albumin (either healthy or CKD-modified) in cell culture medium on active IxS secretion via OAT1 was studied in a novel microfluidic system. To increase clinical relevance of generated *in vitro* data, a quantitative physiologically based translational approach was applied to predict the extent of change in IxS CL_R in CKD relative to the healthy population. IxS was selected as a compound of interest due to

availability of clinical data in both populations, its high extent of binding to albumin in healthy subjects, and the fact that active secretion via OATs contributes predominantly to its renal excretion.

In vitro data on active IxS uptake in ciPTEC-OAT1 showed augmented transporter affinity in the presence of albumin compared to albumin-free condition (Table 2). Increased IxS OAT1 $CL_{int,u}$ was attributed not only to higher IxS affinity for OAT1 but also to increased maximum transporter rates in HSA condition. One possibility is that albumin facilitates access to transporter binding site by overcoming the electrochemical barrier, especially for organic anions. Literature evidence supporting albumin-facilitated transport has mainly focused on hepatic drug transporters.[66,69−71] Albumin-facilitated active transport observed here for IxS indicates relevance of this mechanism for renal OAT1 transporter, but additional mechanistic studies and inclusion of a wider range of drugs (e.g., ranging in fraction bound to albumin, fraction actively secreted by proximal tubule, etc.) are required.

In addition to reduced plasma albumin concentration, CKD is also associated with post-translational guanidinylation of albumin.[15] Guanidinylation appears to cause conformational change in albumin and was proposed as explanation for lower extent of IxS binding to albumin isolated from CKD patients compared to albumin from healthy controls. Rueth et al.[15] suggested that the impact of additional unknown post-translational modifications on binding capacity of albumin in CKD patients might be low. Therefore, CKD-modified albumin synthesized with only guanidinylation post-translational modification in albumin was used in the current study. Our *in vitro* data showed decreased affinity of unbound IxS for OAT1 and a reduction in overall OAT1-mediated uptake $CL_{int,u}$ in the presence of CKD-modified HSA compared to unmodified albumin. Measuring and accounting for IxS binding in different albumin conditions was crucial to avoid bias in interpretation of transporter binding affinity data, as illustrated by the four-fold increase in unbound K_m in CKD-modified HSA relative to HSA condition (Table 2), in contrast to marginal change in uncorrected K_m under the same conditions. Current findings imply that both binding and alteration in albumin-facilitating transport are contributing to decreased IxS uptake via OAT1 in CKD. One possibility is that albumin modification in CKD results in reduced binding capacity, but stronger binding to albumin compared to healthy condition.[15]

Quantitative translation of IxS *in vitro* unbound intrinsic clearance represents the first application of this approach for the transporter kinetic data generated in microfluidic system. IVIVE of data obtained in albumin or CKD-modified albumin condition predicted the observed relative decrease in CL_R in CKD stage IV compared to renal healthy subjects. In the first instance, REF_{OAT1} and PTCPGK physiological scaling factors were kept the same for both healthy and CKD due to lack of quantitative data on these scalars. To address the 20% discrepancy between predicted and observed changes in IxS CL_R, reduction in REF_{OAT1} and PTCPGK as a result of disease was explored in the model. The transporter protein expression (REF_{OAT1}) or tubular cellularity (PTCPGK) were reduced proportional to changes in GFR, in line with the intact nephron hypothesis (Table 6). This approach resulted in excellent agreement between predicted decrease in IxS CL_R in CKD and the clinical observations.

Although the translational approach captured relative decrease in IxS CL_R well, it was apparent that absolute CL_R values in both healthy controls and CKD patients were significantly under-predicted. This under-prediction trend has been reported previously for translation of both hepatic and renal transporter kinetic data.[40,69,72] In the current study, contribution of OAT3 to IxS uptake was not taken into account. The affinity of IxS for OAT3 is 7−10-fold lower relative to OAT1[9,10] and therefore lack of consideration of OAT3 is not anticipated to be a major contributor to the under-prediction trend noted. Existing knowledge gaps or uncertainty in some of the renal physiological parameters and scaling factors, in particular for CKD population, hamper accurate prediction of mechanistic renal drug disposition.[25,29,31] The analysis performed here highlighted sensitivity of the CL_R prediction model to both REF_{OAT1} and PTCPGK values emphasizing the need for accurate determination of these physiological scaling factors for specific patient populations like CKD. Current evidence and data on absolute OAT1 protein abundance in healthy subjects are limited to few studies,[73−75] whereas no OAT1 protein expression data are reported in CKD patients. The importance of determination of OAT1 protein abundance in cell lines used in the microfluidic system to inform the REF scalar is also emphasized.

Evaluation of predictive performance of the *in vitro* data generated in the microfluidic system is also affected by the quality of available *in vivo* data used for comparison. High intra- and intervariability in total/free IxS concentrations was evident in CKD patient groups with similar severity of disease (Table 3, S1). This variability may reflect differing diets, the inflammatory microenvironment and gut microbiota, which may impact IxS production,[76] but may also be related to IxS detection methods used.[77] Ideally, clinical studies should report plasma IxS CL_R in healthy subjects and in specific CKD stages, together with data on the free fractions of IxS in plasma, especially considering that relatively small changes in total concentration of a tightly bound ligand may result in large fluctuations in the free fraction.[78]

In addition to quantitative translational efforts, preliminary studies were performed to mimic complex interplay between uremic solutes and changes in albumin in CKD. ciPTEC-OAT1 cells were perfused with plasma from renal healthy control spiked with IxS or plasma isolated from CKD patients to assess potential combined effects of multiple uremic solutes present in CKD and albumin modifications on OAT1 transporter activity. The preliminary transepithelial transport data showed ability of the microfluidic system to capture reduced overall IxS secretion in uremic plasma relative to renal healthy controls. Further mechanistic studies are required to delineate the impact of individual mechanisms and to investigate quantitative translation of such data. At this stage quantitative translation of transepithelial transport data is not well established due to lack of adequate mechanistic data and corresponding scaling factors.

In conclusion, the findings of the current study support the hypothesis of albumin-facilitated active transport via OAT1. As such, inclusion of albumin in physiologic concentrations is recommended for *in vitro* OAT1 assays, particularly for highly albumin-bound compounds. In addition, current findings highlight the impact of modifications of plasma albumin on active transport of IxS via OAT1 *in vitro*. For the first time, this study applied quantitative translation of transporter kinetic data generated in a novel microfluidic system to a clinically relevant setting and identified important knowledge gaps required for quantitative prediction of renal drug disposition. We envisage that the application of novel microfluidic systems together with mechanistic modeling of *in vitro* data will significantly increase our understanding of underlying processes responsible for the accumulation of uremic toxins and provide valuable input in PBPK models to support model-informed dose recommendations for this patient population.

■ ASSOCIATED CONTENT

ⓢ Supporting Information

The Supporting Information is available free of charge on the ACS Publications website at DOI: 10.1021/acs.molpharmaceut.9b00681.

> Figure S1: determination of IxS fraction unbound in incubation media; Figure S2: cell viability and barrier function upon perfusion; Table S1: studies reporting serum IxS free and total concentrations and fraction unbound in plasma; Table S2: determination of average cell number per fiber; Table S3: reported differences in Q_R parameter between healthy subjects and CKD patients; methods; LC−MS analysis of indoxyl sulfate samples (PDF)

■ AUTHOR INFORMATION

Corresponding Authors
*E-mail: aleksandra.galetin@manchester.ac.uk (A.G.).
*E-mail: R.Masereeuw@uu.nl (R.M.).
ORCID ⓞ
Rosalinde Masereeuw: 0000-0002-1560-1074
Aleksandra Galetin: 0000-0002-3933-5217
Author Contributions
○These senior authors contributed equally to this work.

Notes
The authors declare no competing financial interest.

■ ACKNOWLEDGMENTS

■ ABBREVIATIONS

ciPTEC-OAT1, conditionally immortalized human proximal tubule cells overexpressing OAT1; CL_{intu}, *in vitro* unbound intrinsic clearance; $CL_{intu,scaled}$, scaled *in vivo* unbound intrinsic clearance; CL_R, renal plasma excretion clearance; CKD, chronic kidney disease; F_{reab}, fractional tubular reabsorption; fu_{med}/fu_p, fraction unbound in media/plasma; HSA, human serum albumin; IVIVE, *in vitro- in vivo* extrapolation; IxS, indoxyl sulfate; K_{mu}, unbound transporter affinity; KW_{cortex}, kidney cortex weight; OAT1, organic anion transporter 1; PBPK, physiologically based pharmacokinetic modeling; PTCPGK, proximal tubule cells per g of kidney; Q_R, renal cortex blood flow; $R_{B:P}$, blood-to-plasma ratio; REF, relative expression factor; V_{max}, maximum uptake rate

■ REFERENCES

(1) Bruck, K.; Stel, V. S.; Gambaro, G.; Hallan, S.; Volzke, H.; Arnlov, J.; Kastarinen, M.; Guessous, I.; Vinhas, J.; Stengel, B.; Brenner, H.; Chudek, J.; Romundstad, S.; Tomson, C.; Gonzalez, A. O.; Bello, A. K.; Ferrieres, J.; Palmieri, L.; Browne, G.; Capuano, V.; Van Biesen, W.; Zoccali, C.; Gansevoort, R.; Navis, G.; Rothenbacher, D.; Ferraro, P. M.; Nitsch, D.; Wanner, C.; Jager, K. J. CKD Prevalence Varies across the European General Population. *J. Am. Soc. Nephrol.* **2016**, *27* (7), 2135−47.

(2) United States Renal Data System. Chapter 1 - CKD in the general population. *2018 USRDS Annual Data Report*; National Institutes of Health, National Institute of Diabetes and Digestive and Kidney Diseases: Bethesda, MD, 2018; Vol. *1*. https://www.usrds.org/adr.aspx.

(3) Hsueh, C. H.; Yoshida, K.; Zhao, P.; Meyer, T. W.; Zhang, L.; Huang, S. M.; Giacomini, K. M. Identification and Quantitative Assessment of Uremic Solutes as Inhibitors of Renal Organic Anion Transporters, OAT1 and OAT3. *Mol. Pharmaceutics* **2016**, *13* (9), 3130−40.

(4) Vanholder, R.; Schepers, E.; Pletinck, A.; Nagler, E. V.; Glorieux, G. The uremic toxicity of indoxyl sulfate and p-cresyl sulfate: a systematic review. *J. Am. Soc. Nephrol.* **2014**, *25* (9), 1897−907.

(5) Leong, S. C.; Sirich, T. L. Indoxyl Sulfate-Review of Toxicity and Therapeutic Strategies. *Toxins* **2016**, *8* (12), 358.

(6) Bricker, N. S.; Morrin, P. A.; Kime, S. W., Jr. The pathologic physiology of chronic Bright's disease. An exposition of the "intact nephron hypothesis. *Am. J. Med.* **1960**, *28*, 77−98.

(7) Naud, J.; Michaud, J.; Beauchemin, S.; Hebert, M. J.; Roger, M.; Lefrancois, S.; Leblond, F. A.; Pichette, V. Effects of chronic renal failure on kidney drug transporters and cytochrome P450 in rats. *Drug Metab. Dispos.* **2011**, *39* (8), 1363−9.

(8) Watanabe, H.; Miyamoto, Y.; Otagiri, M.; Maruyama, T. Update on the pharmacokinetics and redox properties of protein-bound uremic toxins. *J. Pharm. Sci.* **2011**, *100* (9), 3682−95.

(9) Enomoto, A.; Takeda, M.; Tojo, A.; Sekine, T.; Cha, S. H.; Khamdang, S.; Takayama, F.; Aoyama, I.; Nakamura, S.; Endou, H.; Niwa, T. Role of organic anion transporters in the tubular transport of indoxyl sulfate and the induction of its nephrotoxicity. *J. Am. Soc. Nephrol.* **2002**, *13* (7), 1711−20.

(10) Deguchi, T.; Kusuhara, H.; Takadate, A.; Endou, H.; Otagiri, M.; Sugiyama, Y. Characterization of uremic toxin transport by organic anion transporters in the kidney. *Kidney Int.* **2004**, *65* (1), 162−74.

(11) Jansen, J.; Fedecostante, M.; Wilmer, M. J.; Peters, J. G.; Kreuser, U. M.; van den Broek, P. H.; Mensink, R. A.; Boltje, T. J.; Stamatialis, D.; Wetzels, J. F.; van den Heuvel, L. P.; Hoenderop, J. G.; Masereeuw, R. Bioengineered kidney tubules efficiently excrete uremic toxins. *Sci. Rep.* **2016**, *6*, 26715.

(12) Mutsaers, H. A.; van den Heuvel, L. P.; Ringens, L. H.; Dankers, A. C.; Russel, F. G.; Wetzels, J. F.; Hoenderop, J. G.; Masereeuw, R. Uremic toxins inhibit transport by breast cancer resistance protein and multidrug resistance protein 4 at clinically relevant concentrations. *PLoS One* **2011**, *6* (4), No. e18438.

(13) Enomoto, A.; Takeda, M.; Taki, K.; Takayama, F.; Noshiro, R.; Niwa, T.; Endou, H. Interactions of human organic anion as well as cation transporters with indoxyl sulfate. *Eur. J. Pharmacol.* **2003**, *466* (1−2), 13−20.

(14) Viaene, L.; Annaert, P.; de Loor, H.; Poesen, R.; Evenepoel, P.; Meijers, B. Albumin is the main plasma binding protein for indoxyl sulfate and p-cresyl sulfate. *Biopharm. Drug Dispos.* **2013**, *34* (3), 165−75.

(15) Rueth, M.; Lemke, H. D.; Preisinger, C.; Krieter, D.; Theelen, W.; Gajjala, P.; Devine, E.; Zidek, W.; Jankowski, J.; Jankowski, V. Guanidinylations of albumin decreased binding capacity of hydrophobic metabolites. *Acta Physiol.* **2015**, *215* (1), 13−23.

(16) Jansen, J.; Jankowski, J.; Gajjala, P. R.; Wetzels, J. F. M.; Masereeuw, R. Disposition and clinical implications of protein-bound uremic toxins. *Clin. Sci.* **2017**, *131* (14), 1631−1647.

(17) Gajjala, P. R.; Fliser, D.; Speer, T.; Jankowski, V.; Jankowski, J. Emerging role of post-translational modifications in chronic kidney disease and cardiovascular disease. *Nephrol., Dial., Transplant.* **2015**, *30* (11), 1814−24.

(18) Pichette, V.; Geadah, D.; du Souich, P. Role of plasma protein binding on renal metabolism and dynamics of furosemide in the rabbit. *Drug Metab. Dispos.* **1999**, *27* (1), 81−5.

(19) Jansen, J.; De Napoli, I. E.; Fedecostante, M.; Schophuizen, C. M.; Chevtchik, N. V.; Wilmer, M. J.; van Asbeck, A. H.; Croes, H. J.; Pertijs, J. C.; Wetzels, J. F.; Hilbrands, L. B.; van den Heuvel, L. P.; Hoenderop, J. G.; Stamatialis, D.; Masereeuw, R. Human proximal tubule epithelial cells cultured on hollow fibers: living membranes that actively transport organic cations. *Sci. Rep.* **2015**, *5*, 16702.

(20) Jones, H. M.; Barton, H. A.; Lai, Y.; Bi, Y. A.; Kimoto, E.; Kempshall, S.; Tate, S. C.; El-Kattan, A.; Houston, J. B.; Galetin, A.; Fenner, K. S. Mechanistic pharmacokinetic modeling for the prediction of transporter-mediated disposition in humans from sandwich culture human hepatocyte data. *Drug Metab. Dispos.* **2012**, *40* (5), 1007−17.

(21) Rostami-Hodjegan, A. Physiologically based pharmacokinetics joined with in vitro-in vivo extrapolation of ADME: a marriage under the arch of systems pharmacology. *Clin. Pharmacol. Ther.* **2012**, *92* (1), 50−61.

(22) Guo, Y.; Chu, X.; Parrott, N. J.; Brouwer, K. L. R.; Hsu, V.; Nagar, S.; Matsson, P.; Sharma, P.; Snoeys, J.; Sugiyama, Y.; Tatosian, D.; Unadkat, J. D.; Huang, S. M.; Galetin, A.; International Transporter, C. Advancing Predictions of Tissue and Intracellular Drug Concentrations Using In Vitro, Imaging and Physiologically Based Pharmacokinetic Modeling Approaches. *Clin. Pharmacol. Ther.* **2018**, *104* (5), 865−889.

(23) Gertz, M.; Cartwright, C. M.; Hobbs, M. J.; Kenworthy, K. E.; Rowland, M.; Houston, J. B.; Galetin, A. Cyclosporine inhibition of hepatic and intestinal CYP3A4, uptake and efflux transporters: application of PBPK modeling in the assessment of drug-drug interaction potential. *Pharm. Res.* **2013**, *30* (3), 761−80.

(24) Badee, J.; Achour, B.; Rostami-Hodjegan, A.; Galetin, A. Meta-analysis of expression of hepatic organic anion-transporting polypeptide (OATP) transporters in cellular systems relative to human liver tissue. *Drug Metab. Dispos.* **2015**, *43* (4), 424−32.

(25) Scotcher, D.; Jones, C.; Posada, M.; Rostami-Hodjegan, A.; Galetin, A. Key to Opening Kidney for In Vitro-In Vivo Extrapolation Entrance in Health and Disease: Part I: In Vitro Systems and Physiological Data. *AAPS J.* **2016**, *18* (5), 1067−81.

(26) Tsamandouras, N.; Chen, W. L. K.; Edington, C. D.; Stokes, C. L.; Griffith, L. G.; Cirit, M. Integrated Gut and Liver Microphysiological Systems for Quantitative In Vitro Pharmacokinetic Studies. *AAPS J.* **2017**, *19* (5), 1499−1512.

(27) Cirit, M.; Stokes, C. L. Maximizing the impact of microphysiological systems with in vitro-in vivo translation. *Lab Chip* **2018**, *18* (13), 1831−1837.

(28) Galetin, A.; Zhao, P.; Huang, S. M. Physiologically Based Pharmacokinetic Modeling of Drug Transporters to Facilitate Individualized Dose Prediction. *J. Pharm. Sci.* **2017**, *106* (9), 2204−2208.

(29) Grimstein, M.; Yang, Y.; Zhang, X.; Grillo, J.; Huang, S. M.; Zineh, I.; Wang, Y. Physiologically Based Pharmacokinetic Modeling in Regulatory Science: An Update From the U.S. Food and Drug Administration's Office of Clinical Pharmacology. *J. Pharm. Sci.* **2019**, *108* (1), 21−25.

(30) Tan, M. L.; Zhao, P.; Zhang, L.; Ho, Y. F.; Varma, M. V. S.; Neuhoff, S.; Nolin, T. D. Use of Physiologically Based Pharmacokinetic Modeling to Evaluate the Effect of Chronic Kidney Disease on the Disposition of Hepatic CYP2C8 and OATP1B Drug Substrates. *Clin. Pharmacol. Ther.* **2019**, *105* (3), 719−729.

(31) Scotcher, D.; Jones, C. R.; Galetin, A.; Rostami-Hodjegan, A. Delineating the Role of Various Factors in Renal Disposition of Digoxin through Application of Physiologically Based Kidney Model to Renal Impairment Populations. *J. Pharmacol. Exp. Ther.* **2017**, *360* (3), 484−495.

(32) Hsu, V.; de, L. T. V. M.; Zhao, P.; Zhang, L.; Zheng, J. H.; Nordmark, A.; Berglund, E. G.; Giacomini, K. M.; Huang, S. M. Towards quantitation of the effects of renal impairment and probenecid inhibition on kidney uptake and efflux transporters, using physiologically based pharmacokinetic modelling and simulations. *Clin. Pharmacokinet.* **2014**, *53* (3), 283–293.

(33) Hsueh, C. H.; Hsu, V.; Zhao, P.; Zhang, L.; Giacomini, K. M.; Huang, S. M. PBPK Modeling of the Effect of Reduced Kidney Function on the Pharmacokinetics of Drugs Excreted Renally by Organic Anion Transporters. *Clin. Pharmacol. Ther.* **2018**, *103* (3), 485–492.

(34) Nieskens, T. T.; Peters, J. G.; Schreurs, M. J.; Smits, N.; Woestenenk, R.; Jansen, K.; van der Made, T. K.; Roring, M.; Hilgendorf, C.; Wilmer, M. J.; Masereeuw, R. A Human Renal Proximal Tubule Cell Line with Stable Organic Anion Transporter 1 and 3 Expression Predictive for Antiviral-Induced Toxicity. *AAPS J.* **2016**, *18* (2), 465–75.

(35) Jansen, J.; Schophuizen, C. M.; Wilmer, M. J.; Lahham, S. H.; Mutsaers, H. A.; Wetzels, J. F.; Bank, R. A.; van den Heuvel, L. P.; Hoenderop, J. G.; Masereeuw, R. A morphological and functional comparison of proximal tubule cell lines established from human urine and kidney tissue. *Exp. Cell Res.* **2014**, *323* (1), 87–99.

(36) Neuhoff, S.; Gaohua, L.; Burt, H.; Jamei, M.; Li, L.; Tucker, G.; Rostami-Hodjegan, A. Accounting for Transporters in Renal Clearance: Towards a Mechanistic Kidney Model (Mech KiM). In *Transporters in Drug Development. Discovery, Optimization, Clinical Study and Regulation*; Steffansen, Y. S. B., Ed.; Springer Science+Business Media: New York, 2013; pp 155–77.

(37) Habu, Y.; Yano, I.; Takeuchi, A.; Saito, H.; Okuda, M.; Fukatsu, A.; Inui, K. Decreased activity of basolateral organic ion transports in hyperuricemic rat kidney: roles of organic ion transporters, rOAT1, rOAT3 and rOCT2. *Biochem. Pharmacol.* **2003**, *66* (6), 1107–14.

(38) Forbes, M. S.; Thornhill, B. A.; Minor, J. J.; Gordon, K. A.; Galarreta, C. I.; Chevalier, R. L. Fight-or-flight: murine unilateral ureteral obstruction causes extensive proximal tubular degeneration, collecting duct dilatation, and minimal fibrosis. *Am. J. Physiol. Renal Physiol.* **2012**, *303* (1), F120–9.

(39) Deguchi, T.; Takemoto, M.; Uehara, N.; Lindup, W. E.; Suenaga, A.; Otagiri, M. Renal clearance of endogenous hippurate correlates with expression levels of renal organic anion transporters in uremic rats. *J. Pharmacol. Exp. Ther.* **2005**, *314* (2), 932–8.

(40) Zamek-Gliszczynski, M. J.; Lee, C. A.; Poirier, A.; Bentz, J.; Chu, X.; Ellens, H.; Ishikawa, T.; Jamei, M.; Kalvass, J. C.; Nagar, S.; Pang, K. S.; Korzekwa, K.; Swaan, P. W.; Taub, M. E.; Zhao, P.; Galetin, A. ITC recommendations for transporter kinetic parameter estimation and translational modeling of transport-mediated PK and DDIs in humans. *Clin. Pharmacol. Ther.* **2013**, *94* (1), 64–79.

(41) Yang, J.; Jamei, M.; Yeo, K. R.; Rostami-Hodjegan, A.; Tucker, G. T. Misuse of the well-stirred model of hepatic drug clearance. *Drug Metab. Dispos.* **2007**, *35* (3), 501–2.

(42) Rowland Yeo, K.; Aarabi, M.; Jamei, M.; Rostami-Hodjegan, A. Modeling and predicting drug pharmacokinetics in patients with renal impairment. *Expert Rev. Clin. Pharmacol.* **2011**, *4* (2), 261–74.

(43) Duranton, F.; Cohen, G.; De Smet, R.; Rodriguez, M.; Jankowski, J.; Vanholder, R.; Argiles, A. Normal and pathologic concentrations of uremic toxins. *J. Am. Soc. Nephrol.* **2012**, *23* (7), 1258–70.

(44) Rossi, M.; Campbell, K.; Johnson, D.; Stanton, T.; Pascoe, E.; Hawley, C.; Dimeski, G.; McWhinney, B.; Ungerer, J.; Isbel, N. Uraemic toxins and cardiovascular disease across the chronic kidney disease spectrum: an observational study. *Nutr., Metab. Cardiovasc. Dis.* **2014**, *24* (9), 1035–42.

(45) Molina, D. K.; DiMaio, V. J. Normal organ weights in men: part II-the brain, lungs, liver, spleen, and kidneys. *Am. J. Forensic Med. Pathol.* **2012**, *33* (4), 368–72.

(46) Molina, D. K.; DiMaio, V. J. Normal Organ Weights in Women: Part II-The Brain, Lungs, Liver, Spleen, and Kidneys. *Am. J. Forensic Med. Pathol.* **2015**, *36* (3), 182–7.

(47) Poesen, R.; Viaene, L.; Verbeke, K.; Claes, K.; Bammens, B.; Sprangers, B.; Naesens, M.; Vanrenterghem, Y.; Kuypers, D.; Evenepoel, P.; Meijers, B. Renal clearance and intestinal generation of p-cresyl sulfate and indoxyl sulfate in CKD. *Clin. J. Am. Soc. Nephrol.* **2013**, *8* (9), 1508–14.

(48) Scotcher, D.; Billington, S.; Brown, J.; Jones, C. R.; Brown, C. D. A.; Rostami-Hodjegan, A.; Galetin, A. Microsomal and Cytosolic Scaling Factors in Dog and Human Kidney Cortex and Application for In Vitro-In Vivo Extrapolation of Renal Metabolic Clearance. *Drug Metab. Dispos.* **2017**, *45* (5), 556–568.

(49) Chapter 1: Definition and classification of CKD. *Kidney Int. Suppl.* **2013**, *3*, (1), 19–62.

(50) Shafi, T.; Sirich, T. L.; Meyer, T. W.; Hostetter, T. H.; Plummer, N. S.; Hwang, S.; Melamed, M. L.; Banerjee, T.; Coresh, J.; Powe, N. R. Results of the HEMO Study suggest that p-cresol sulfate and indoxyl sulfate are not associated with cardiovascular outcomes. *Kidney Int.* **2017**, *92* (6), 1484–1492.

(51) Camacho, O.; Rosales, M. C.; Shafi, T.; Fullman, J.; Plummer, N. S.; Meyer, T. W.; Sirich, T. L. Effect of a sustained difference in hemodialytic clearance on the plasma levels of p-cresol sulfate and indoxyl sulfate. *Nephrol., Dial., Transplant.* **2016**, *31* (8), 1335–41.

(52) Rossi, M.; Johnson, D. W.; Morrison, M.; Pascoe, E. M.; Coombes, J. S.; Forbes, J. M.; Szeto, C. C.; McWhinney, B. C.; Ungerer, J. P.; Campbell, K. L. Synbiotics Easing Renal Failure by Improving Gut Microbiology (SYNERGY): A Randomized Trial. *Clin. J. Am. Soc. Nephrol.* **2016**, *11* (2), 223–31.

(53) Eloot, S.; Vanholder, R.; Dequidt, C.; Van Biesen, W. Removal of Different Classes of Uremic Toxins in APD vs CAPD: A Randomized Cross-Over Study. *Peritoneal Dial. Int.* **2015**, *35* (4), 436–42.

(54) Shafi, T.; Meyer, T. W.; Hostetter, T. H.; Melamed, M. L.; Parekh, R. S.; Hwang, S.; Banerjee, T.; Coresh, J.; Powe, N. R. Free Levels of Selected Organic Solutes and Cardiovascular Morbidity and Mortality in Hemodialysis Patients: Results from the Retained Organic Solutes and Clinical Outcomes (ROSCO) Investigators. *PLoS One* **2015**, *10* (5), No. e0126048.

(55) Sirich, T. L.; Plummer, N. S.; Gardner, C. D.; Hostetter, T. H.; Meyer, T. W. Effect of increasing dietary fiber on plasma levels of colon-derived solutes in hemodialysis patients. *Clin. J. Am. Soc. Nephrol.* **2014**, *9* (9), 1603–10.

(56) Wu, I. W.; Hsu, K. H.; Sun, C. Y.; Tsai, C. J.; Wu, M. S.; Lee, C. C. Oral adsorbent AST-120 potentiates the effect of erythropoietin-stimulating agents on Stage 5 chronic kidney disease patients: a randomized crossover study. *Nephrol., Dial., Transplant.* **2014**, *29* (9), 1719–27.

(57) Lin, C. J.; Pan, C. F.; Chuang, C. K.; Liu, H. L.; Sun, F. J.; Wang, T. J.; Chen, H. H.; Wu, C. J. Gastrointestinal-related uremic toxins in peritoneal dialysis: a pilot study with a 5-year follow-up. *Arch. Med. Res.* **2013**, *44* (7), 535–41.

(58) *The European Uremic Toxins Database*; European Soociety for Artificial Organs, 2019. www.uremic-toxins.org (accessed May 16, 2019).

(59) Sirich, T. L.; Aronov, P. A.; Plummer, N. S.; Hostetter, T. H.; Meyer, T. W. Numerous protein-bound solutes are cleared by the kidney with high efficiency. *Kidney Int.* **2013**, *84* (3), 585–90.

(60) Suchy-Dicey, A. M.; Laha, T.; Hoofnagle, A.; Newitt, R.; Sirich, T. L.; Meyer, T. W.; Thummel, K. E.; Yanez, N. D.; Himmelfarb, J.; Weiss, N. S.; Kestenbaum, B. R. Tubular Secretion in CKD. *J. Am. Soc. Nephrol.* **2016**, *27* (7), 2148–55.

(61) Rivara, M. B.; Zelnick, L. R.; Hoofnagle, A. N.; Newitt, R.; Tracy, R. P.; Kratz, M.; Weigle, D. S.; Kestenbaum, B. R. Diurnal and Long-term Variation in Plasma Concentrations and Renal Clearances of Circulating Markers of Kidney Proximal Tubular Secretion. *Clin. Chem.* **2017**, *63* (4), 915–923.

(62) Posada, M. M.; Cannady, E. A.; Payne, C. D.; Zhang, X.; Bacon, J. A.; Pak, Y. A.; Higgins, J. W.; Shahri, N.; Hall, S. D.; Hillgren, K. M. Prediction of Transporter-Mediated Drug-Drug Interactions for Baricitinib. *Clin. Transl. Sci.* **2017**, *10* (6), 509–519.

(63) Ball, K.; Jamier, T.; Parmentier, Y.; Denizot, C.; Mallier, A.; Chenel, M. Prediction of renal transporter-mediated drug-drug interactions for a drug which is an OAT substrate and inhibitor using PBPK modelling. *Eur. J. Pharm. Sci.* **2017**, *106*, 122−132.

(64) Mathialagan, S.; Piotrowski, M. A.; Tess, D. A.; Feng, B.; Litchfield, J.; Varma, M. V. Quantitative Prediction of Human Renal Clearance and Drug-Drug Interactions of Organic Anion Transporter Substrates Using In Vitro Transport Data: A Relative Activity Factor Approach. *Drug Metab. Dispos.* **2017**, *45* (4), 409−417.

(65) Feng, B.; Hurst, S.; Lu, Y.; Varma, M. V.; Rotter, C. J.; El-Kattan, A.; Lockwood, P.; Corrigan, B. Quantitative prediction of renal transporter-mediated clinical drug-drug interactions. *Mol. Pharmaceutics* **2013**, *10* (11), 4207−15.

(66) Weisiger, R.; Gollan, J.; Ockner, R. Receptor for albumin on the liver cell surface may mediate uptake of fatty acids and other albumin-bound substances. *Science* **1981**, *211* (4486), 1048−51.

(67) Mao, J.; Mohutsky, M. A.; Harrelson, J. P.; Wrighton, S. A.; Hall, S. D. Predictions of cytochrome P450-mediated drug-drug interactions using cryopreserved human hepatocytes: comparison of plasma and protein-free media incubation conditions. *Drug Metab. Dispos.* **2012**, *40* (4), 706−16.

(68) Wilkinson, G. R. Clearance approaches in pharmacology. *Pharmacol. Rev.* **1987**, *39* (1), 1−47.

(69) Kim, S. J.; Lee, K. R.; Miyauchi, S.; Sugiyama, Y. Extrapolation of In Vivo Hepatic Clearance from In Vitro Uptake Clearance by Suspended Human Hepatocytes for Anionic Drugs with High Binding to Human Albumin: Improvement of In Vitro-to-In Vivo Extrapolation by Considering the "Albumin-Mediated" Hepatic Uptake Mechanism on the Basis of the "Facilitated-Dissociation Model. *Drug Metab. Dispos.* **2019**, *47* (2), 94−103.

(70) Poulin, P.; Haddad, S. Extrapolation of the Hepatic Clearance of Drugs in the Absence of Albumin In Vitro to That in the Presence of Albumin In Vivo: Comparative Assessement of 2 Extrapolation Models Based on the Albumin-Mediated Hepatic Uptake Theory and Limitations and Mechanistic Insights. *J. Pharm. Sci.* **2018**, *107* (7), 1791−1797.

(71) Miyauchi, S.; Masuda, M.; Kim, S. J.; Tanaka, Y.; Lee, K. R.; Iwakado, S.; Nemoto, M.; Sasaki, S.; Shimono, K.; Tanaka, Y.; Sugiyama, Y. The Phenomenon of Albumin-Mediated Hepatic Uptake of Organic Anion Transport Polypeptide Substrates: Prediction of the In Vivo Uptake Clearance from the In Vitro Uptake by Isolated Hepatocytes Using a Facilitated-Dissociation Model. *Drug Metab. Dispos.* **2018**, *46* (3), 259−267.

(72) Menochet, K.; Kenworthy, K. E.; Houston, J. B.; Galetin, A. Use of mechanistic modeling to assess interindividual variability and interspecies differences in active uptake in human and rat hepatocytes. *Drug Metab. Dispos.* **2012**, *40* (9), 1744−56.

(73) Basit, A.; Radi, Z.; Vaidya, V. S.; Karasu, M.; Prasad, B. Kidney Cortical Transporter Expression across Species Using Quantitative Proteomics. *Drug Metab. Dispos.* **2019**, *47* (8), 802−808.

(74) Li, C. Y.; Hosey-Cojocari, C.; Basit, A.; Unadkat, J. D.; Leeder, J. S.; Prasad, B. Optimized Renal Transporter Quantification by Using Aquaporin 1 and Aquaporin 2 as Anatomical Markers: Application in Characterizing the Ontogeny of Renal Transporters and Its Correlation with Hepatic Transporters in Paired Human Samples. *AAPS J.* **2019**, *21* (5), 88.

(75) Cheung, K. W. K.; van Groen, B. D.; Spaans, E.; van Borselen, M. D.; de Bruijn, A.; Simons-Oosterhuis, Y.; Tibboel, D.; Samsom, J. N.; Verdijk, R. M.; Smeets, B.; Zhang, L.; Huang, S. M.; Giacomini, K. M.; de Wildt, S. N. A Comprehensive Analysis of Ontogeny of Renal Drug Transporters: mRNA Analyses, Quantitative Proteomics, and Localization. *Clin. Pharmacol. Ther.* **2019**. DOI: 10.1002/cpt.1516

(76) Evenepoel, P.; Poesen, R.; Meijers, B. The gut-kidney axis. *Pediatr. Nephrol.* **2017**, *32* (11), 2005−2014.

(77) Evenepoel, P.; Glorieux, G.; Meijers, B. p-cresol sulfate and indoxyl sulfate: some clouds are gathering in the uremic toxin sky. *Kidney Int.* **2017**, *92* (6), 1323−1324.

(78) Meijers, B. K.; Bammens, B.; Verbeke, K.; Evenepoel, P. A review of albumin binding in CKD. *Am. J. Kidney Dis.* **2008**, *51* (5), 839−50.